QUANTIFICATION OF STRUCTURE FOR HIGH THERMAL CONDUCTIVITY FIBERS

K. E. Robinson and D. D. Edie
Department of Chemical Engineering, Clemson University, Clemson, South Carolina 29634, USA.

INTRODUCTION

In this work the complementary techniques of high resolution scanning electron microscopy (HRSEM), transmission electron microscopy (TEM) and wide angle x-ray diffraction (WAXD) were used to obtain structural information such as the arrangement, shape and size of graphite crystallites within two different pitch-based carbon fibers. Although the structural information obtained by WAXD is quantitative in nature, the information obtained by the electron microscopy techniques is qualitative. Thus to increase the applicability of this qualitative structural information and more accurately relate it to the fibers' heat transfer and processing properties, a simple image analysis program was developed to quantify the information. This paper describes the image analysis program set-up and presents the initial results obtained using this imaging technique, as well as other structural information on the fibers.

EXPERIMENTAL PROCEDURE

Two sets of ribbon-shaped fibers, melt spun under similar conditions using the same spinnerette and two different pitch precursors (a petroleum-based, heat-soaked mesophase (Fiber A) and a synthetic naphthalene-based mesophase (Fiber B)) were studied in this work. The specific processing conditions used to manufacture these fibers are given elsewhere (1). The axial thermal conductivities of the fibers were estimated from measurements of their electrical resistivities (1, 2). The structures of the fibers were analyzed using HRSEM, TEM and WAXD (1). Finally, an image analysis program was used to quantify qualitative structural information, such as HRSEM images, 002 dark-field images and selected area electron diffraction (SAED) patterns, obtained from the electron microscopy study of the fibers.

The image analysis system consisted of a video camera and frame grabber board, which digitized the respective images and patterns and then transferred this information to the color monitor of a Model IIci Macintosh computer. A public domain program (Image) was used to process and analyze the digital images. Using this image analysis software program, profile plots of pixel gray-levels from equatorial scans (perpendicular to the fiber axis direction) of the SAED patterns were obtained. It should be noted that the fiber sections used in the SAED analysis were given a 2nm coating of gold, which provided an in-situ calibration standard for the determination of interlayer spacings (d_{002}). The diameters of the gold and diffraction rings were calculated from measurements taken from these equatorial density plots. Once the diameters of the gold diffraction rings were known, the magnification factor of the TEM could be calculated (3). Given this information, 002 interlayer spacings could be determined at selected areas within the particular fibers. Similar density plots were conducted on the 002 dark-field images. The images were scanned perpendicular to the fiber axis direction, and the resultant plots were used to give a quantitative measurement of fold-separation parallel to the fiber axis as well as stack heights (Lc values) within the respective fibers. Stack heights were measured from FWHM of the peaks in these plots. Additionally, using the measurement tool of the image analysis program, extensions (La values) of the bright diffracting regions in the dark-field images were computed. Finally, the measurement tool was used to determine fold separations within HRSEM images of the fibers' graphitic sheet structure.

RESULTS

The measured electrical resistivities of Fiber A and B are 7.87$\mu\Omega$-m and 4.55$\mu\Omega$-m, respectively. These values indicate that the thermal conductivitiy of Fiber B should be more than double that of Fiber A (Fiber A has an estimated thermal conductivity of 126W/mK and Fiber B 323W/mK). Figures 1A and 1B show 002 dark-field images taken from longitudinal sections of Fibers A and B, respectively. In both fiber types the diffracting crystallites are aligned along the fiber axis, as is evident by the bright bands running parallel to the fiber axis. However, there is a distinct difference in the degree of preferred orientation and arrangement of the basal crystallites in the two fiber types. In Fiber B the crystallites are more randomly arranged parallel to the fiber axis, whereas in Fiber B there is a definite alignment of the diffracting crystallites in the axial direction. Similar differences in the structures of Fibers A and B were also evident in the HRSEM images taken from the surface skin of these fibers (1). SAED patterns taken from small areas within longitudinal sections further support these differences (1). It was clear from the sharp spot pattern of the 002 layers in the SAED pattern of Fiber B, compared to the arc arrangement in the pattern of Fiber A, that Fiber B has a much higher degree of preferred orientation than Fiber A, which has a more turbostratic structure.

Representative density plots generated from scans of the 002 dark-field images of Fibers A and B are shown in Figures 2A and 2B. It should be noted that these scans are taken perpendicular to the fiber axis direction. Therefore, the distinctive peaks in these plots represent the bright regions where the stacking of the 002 basal layer planes is parallel to the electron beam, whereas regions between the peaks represent areas where the basal planes are perpendicular to the electron beam. In other words, the number of peaks gives an indication of degree of folding parallel to the fiber axis. Additionally, divided or shouldered peaks denote where the bright bands are divided into smaller diffracting regions. The density plots indicate that the degree of folding parallel to the fiber axis is similar for the two fiber types. Fold separations in Fiber A ranged from 12 to 138nm (with an average of 38 ± 18) and in Fiber B from 18 to 200nm (with an average of 57 ± 23nm). However, there does appear to be a difference in the complexity of the peaks in the density plots of the two different fibers. The peaks in the density plot of Fiber A appear to be slightly more complex (more divided and shouldered peaks) than those in the plot of

Fiber B. This difference in the complexity of the peaks could be related to the intertwining of the axial folds in Fiber A. This pattern may cause the bright bands in the 002 dark-field images to be divided into smaller diffracting regions. The diffracting bands in the 002 dark-field images of Fiber B showed fewer of these smaller diffracting regions, implying that the axial folds of Fiber B were more aligned and the crystallites more perfect than those of Fiber A.

Table 1 gives the structural parameters of the ribbon fibers obtained from the TEM imaging analysis technique and WAXD. Although discrepancies exist between certain x-ray and TEM results, specific trends are apparent (1). Fiber B has a lower interlayer spacings and larger, more well-developed crystallites than Fiber A. This indicates that the naphthalene-based mesophase fiber was graphitized to a greater degree and, thus, has a structure more conducive to high thermal conductivity.

CONCLUSIONS

It was found that the naphthalene-based mesophase offered certain advantages as a precursor for fibers with superior heat transfer properties. Fibers melt spun from the synthetic precursor had higher degrees of preferred orientation, graphitization and thermal conductivities than those fibers melt spun from the heat-soaked mesophase. Essentially this research has shown that a more fundamental knowledge of structure-property/processing relationships can be gained by quantifying, qualitative electron microscopy information.

REFERENCES

1. K. E. Robinson and D. D. Edie, submitted to *Carbon* (1995).
2. J. G. Lavin, D. R. Boyington, J. Lahijari, B. Nysten and J. P. Issi, *Carbon* **31** (6), 1002 (1993).
3. D. L. Misel and E. B. Brown, in *Electron Diffraction for Biologists* (Edited by A. D. Glauret), 65-69, New York (1987)

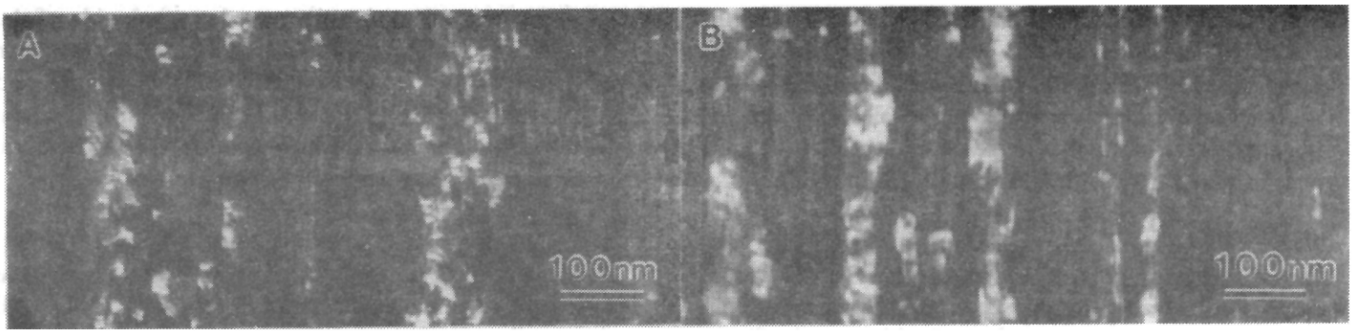

Figure 1. 002 Dark-field images taken from longitudinal sections of (A) Fiber A and (B) Fiber B.

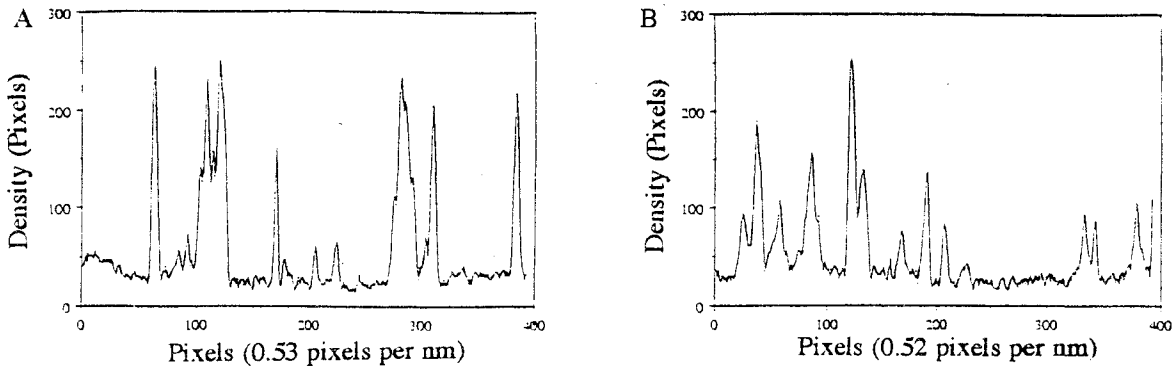

Figure 2. Density plots generated from scans of 002 dark-field images of (A) Fiber A and (B) Fiber B.

Table 1. Structural parameters of ribbon-shaped fibers as obtained from TEM and WAXD analysis.

Fiber Type	TEM			X-Ray Diffraction		
	Interlayer spacing, d_{002} (Å)	Stack height, L_c (Å)	Coherence length, L_a (Å)	Interlayer spacing, d_{002} (Å)	Stack height, L_c (Å)	Coherence length, L_a (Å)
A	3.430 ± 0.007 [1]	116 ± 14	<150	3.411 ± 0.004	123 ± 7	* [2]
B	3.403 ± 0.005	154 ± 16	150-350	3.396 ± 0.004	123 ± 7	282 ± 20

[1] Represents a 95% confidence interval.

[2] 110 and 100 peaks to diffuse to accurately measure La of strand sample.